

Progress in a new conjunction and threat warning service for Space Situational Awareness

James C. S. Bennett, Michael Lachut

*EOS Space Systems Pty Ltd, Queanbeyan NSW Australia
Space Environment Research Centre, Mount Stromlo ACT Australia*

Daniel Kucharski

*Space Environment Research Centre, Mount Stromlo ACT Australia
University of Texas at Austin, Austin TX, USA*

Sven Flegel, Marek Möckel

Space Environment Research Centre, Mount Stromlo ACT Australia

James Allworth, David Kooymans, Alex Pollard, Craig Smith

EOS Space Systems Pty Ltd, Queanbeyan NSW Australia

Joseph O’Leary, Hansani Thanippuli Kankanamalage

Space Environment Research Centre, Mount Stromlo ACT Australia

University of South Australia, SA Australia

Richard Samuel

*Space Environment Research Centre, Mount Stromlo ACT Australia
ANU University, Canberra ACT Australia*

ABSTRACT

This paper reports the progress of the development of a new conjunction and threat warning service for satellite operators and a laser manoeuvre demonstration. The status and characteristics of the network of sensors being used is described and the progress of the space situational awareness service being developed is provided along with a timeline for full operational capability.

The construction of a new site in Learmonth Western Australia – a joint venture between EOS Space Systems and Lockheed Martin, with support from the Australian Department of Defence – sees new optical and laser ranging systems installed to supplement EOS’s existing site at Mt Stromlo, Canberra. Four telescopes have been installed at Learmonth: two 1-metre laser beam directors and two 0.7 metre Deep Space Trackers. The installation of a 0.7 metre Deep Space Tracker by EOS Space Systems for the Space Environment Research Centre (SERC) at Mount Stromlo, supplements EOS’s existing 1.8 metre Space Debris Tracking System.

The sensor network is automated and can be adapted from day-to-day tasking to perform custom mission requests and ad-hoc tasking, for example, facilitating tasking from external organisations for observation collection. An information gain based scheduler is also being developed. An example of a typical daily mission cycle is: perform an all-on-all conjunction assessments, schedule the sensors to collect observations on the objects of interest, correlate the tracks with known objects, generate new orbital elements by fitting the collected observations, and re-task the sensors based on a new conjunction assessment. During a session the telescope domes will open and perform the tasking automatically and shut down and close when the session has finished.

At SERC the goal is to contribute to the mitigation of the debris environment by using high powered continuous wave lasers to apply photon pressure to perturb objects on orbit so that they avoid a collision. To demonstrate this goal, several operational components are needed to ensure a debris object is not moved into a less favourable trajectory, for example, after perturbing the orbit there is a higher chance of collision. This requires knowledge of all objects and their behaviour in the vicinity of the demonstration. The space situational awareness system is the culmination of a number of research programs.

SERC are developing a catalogue utilising the tracking data collected by the sensor network described above. Within the catalogue are object states and covariances as well as object characteristics. Traceability of catalogue change events has been an important component of the development and has been designed to facilitate the research developments being developed in SERC as they come into fruition. The development of high-rate photometric light

sampling methods allow for the object's spin characteristics to be estimated, as well as albedo, optical cross-section, and other object characteristics and behaviours. The passive and active tracking observations are all stored in a tracks database and correlated with objects, with the uncorrelated tracks stored for later assessment and correlation. The orbit element generation process is performed using a Batch Least Squares process, numerically integrating the equations of motion. The main perturbing forces are present in the force model and at the moment the automated element generation assumes a spherical object. Future enhancements will see non-spherical objects considered in the automated element generation.

The conjunction assessments have been parallelised to run efficiently on a GPU with a propagator interface allowing the use of different propagators. The software has been developed so that it is multi-platform. Nonlinear and non-Gaussian error propagation has also been developed within SERC and provides more realistic collision probability assessments, and the prediction in the breakdown of Gaussianity.

Information on the catalogue status, size and accuracy is reported as well as the integration and deployment of the conjunction and threat warning services.

1. INTRODUCTION

The near-Earth space environment is becoming increasingly congested. With several companies planning to launch mega-constellations into low-Earth orbit, these will challenge the existing debris mitigation practices, and conjunction warnings will be more frequent. Accurate and timely conjunction warnings will be necessary. Mitigation and remediation methods have been investigated and studies suggest that active debris removal is necessary to reverse the trend in the growth of the space debris field.

The Space Environment Research Centre (SERC) seeks to assist in curbing the growth of the debris field by building continuous wave laser systems to nudge space debris so that a collision is avoided. The method will use high-powered CW lasers coupled with adaptive optics to deliver photon pressure to an object to remotely manoeuvre it from a collision path. The program is challenging but if successful it can buy time until the active debris removal missions can remove mass from orbit. A critical prerequisite component of this mission is good space situational and domain awareness, awareness that the public catalogues can't currently provide.

This paper reports on the progress made within the Space Asset Management program in SERC, also known as Research Program 3 (RP3), on a conjunction and threat warning (CATW) capability. Several advancements in the research and development of the capability have been achieved and the following areas are covered in this paper:

1. The automated sensor network;
2. The new space object database and catalogue;
3. Track correlations;
4. Object characterization;
5. Orbit ephemeris generation and propagation;
6. Sensor scheduling;
7. Parallelised conjunction assessments;
8. Nonlinear + non-Gaussian error propagation

Following these, a description of the other research areas currently being pursued in post graduate study programs is provided. Finally, a timeline for the full operational capability is reported. This work forms a critical component to realise the laser manoeuvre capability.

2. SENSORS

The location of the Mount Stromlo (site A) and Learmonth (site B) sites is shown in Fig. 1. EOS Space System' Space Debris Tracking Station at Mt Stromlo site was recommissioned in 2004 following the bushfires in 2003 that destroyed the facility. The site features a 1.8 metre alt/az telescope equipped with both passive and active debris tracking systems. The on-sky telescope mount pointing accuracy is 1–3 arc-seconds RMS. The system is equipped with a high power pulsed laser system for debris tracking [1], which has a range accuracy of ~1.5 metres. The system is capable of both passive tracking in LEO-to-GEO and beyond, and active laser ranging to objects without

retro reflectors for LEO. For objects with retro reflectors the accurate laser range measurements can be collected in LEO-to-GEO and beyond.

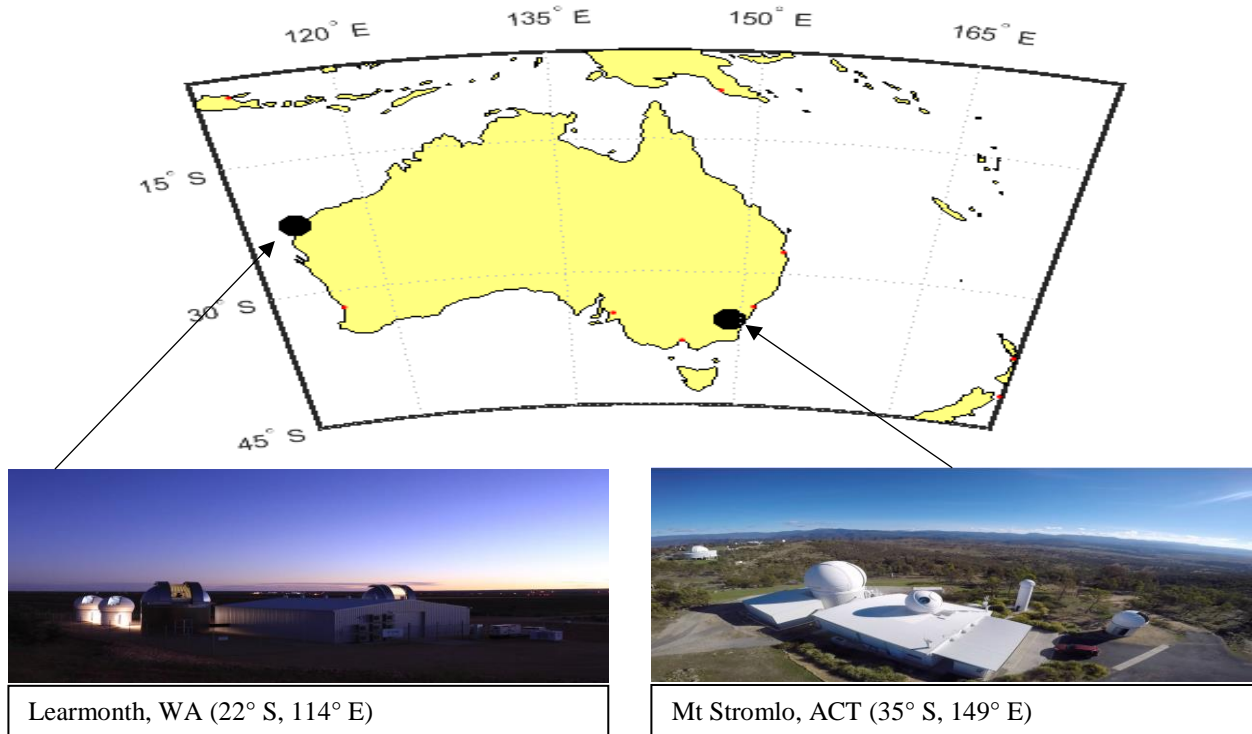


Fig. 1. Map showing the locations of the sensors

Also located at Mount Stromlo is a newly-integrated 0.7 metre telescope, primarily for tracking objects in higher orbits but is also capable of tracking LEO objects. The system is passive with a rotating tertiary mirror to select sensors mounted on the Nasmyth ports. The system features a CCD tracking camera on one port and a high-rate photodetector on the other port for object characterisation studies.

The Learmonth site – a joint venture between EOS Space Systems and Lockheed Martin Australia, with support from the Australian Department of Defence – has two 1 metre telescopes and two 0.7 metre telescopes. The 1 metre systems are active and passive tracking sensors and the 0.7 metre telescopes are passive. A summary of the network configuration is shown in Tab. 1.

Tab. 1. General configuration of the network

System ID	Site	Aperture	Configuration
A1	Mt Stromlo	1.8 m	Active + Passive
A2	Mt Stromlo	0.7 m	Passive
B1	Learmonth	1.0 m	Active + Passive
B2	Learmonth	1.0 m	Active + Passive
B3	Learmonth	0.7 m	Passive
B4	Learmonth	0.7 m	Passive

The sensor network sites are unmanned and run autonomously. In the event of bad weather such as persistent cloud, rain on approach, etc., the systems will pause the tracking session and close the domes. Once the weather clears, the system will automatically reopen the telescope enclosures and resume tasking.

2.1 Sensor Tasking

The sensor network can be tasked in several ways, each with a different operational focus and EOS have spent over 10 years developing automated sensor tasking. SERC has developed a multi-sensor information gain based scheduler [2, 3] for the network has been tested at Stromlo and interfaces have been generated by EOS Space Systems to parse the schedule generated by the SERC scheduler. Under contract to SERC, Industrial Sciences Group¹ have extended the functionality of the scheduler which now efficiently distributes passive and active tasking across the sensor network, maximizing the information gain.

3. DATABASE & CATALOGUE

To realize an operational conjunction assessment and threat warning capability a central database-backed application was created to manage the storage, association and processing of tracking data. This application protects the integrity of the underlying relational database, ensuring that as data is added it is linked to reference data such as a track to its origin telescope and the satellite that the track is believed to be of. In the case of an orbit determination, all of the used tracks are linked, as well as the earth orientation parameters, solar flux data, the force models used and both known and estimated characteristics of the satellite. When the orbital determination is finished its status, as well as reports and resulting element are then added to the database so they can be used for cueing sensors, determining the accuracy of a telescope and other analyses. This ability to see the origin of all data and which data was used in what processing is a key element of the application and its database.

The application allows access to the database via HTTP and has a small html front end to allow for easy access. The HTTP interface allows data scientists and engineers to build other processing applications with existing libraries in a language agnostic way rather than being bound to in house tooling and C++. To this end, visualisations and techniques for analysing the data can be quickly built to experiment with the data stored without fear of interfering with the database's integrity.

The database currently contains over 60,000 observation passes and over 6,000 orbital ephemerides and is growing rapidly (over 20,000 observation passes added since June 2018). The objects span all near-Earth orbital types and the catalogue will grow quickly due to Learmonth meeting the expected performance measures². The Mount Stromlo site has been focused on the research development integration and testing. It will also contribute data into the catalogue, but not at the operational rate that Learmonth provides.

4. TRACK CORRELATIONS

Once a track has been collected it is sent to the post processing server where the raw tracks are correlated with known objects. If the object fails to be correlated it is then tagged as an uncorrelated track and doesn't enter into the orbit determination process. The uncorrelated tracks are then re-analysed and correlated to objects in the object database. To perform the track correlation an existing state vector and covariance matrix are used and both are propagated using the numerical integration procedure outlined in Section 6. Each observation is validated using probabilistic data association. In the event there is no a priori state vector and covariance in the catalogue, the process reverts to a state vector and covariance determined by fitting pseudo-observations generated using SGP4 from multiple TLEs. This method is called the TLE-OD method. The TLE at the start of the OD span is used as the initial state for the batch least squares fitting to generate the multi-TLE fit.

If there is not a pre-determined TLE-OD then the process reverts back to a single TLE with a nominal error covariance matrix. The SGP4 propagator is used to propagate the state.

5. OBJECT CHARACTERISATION

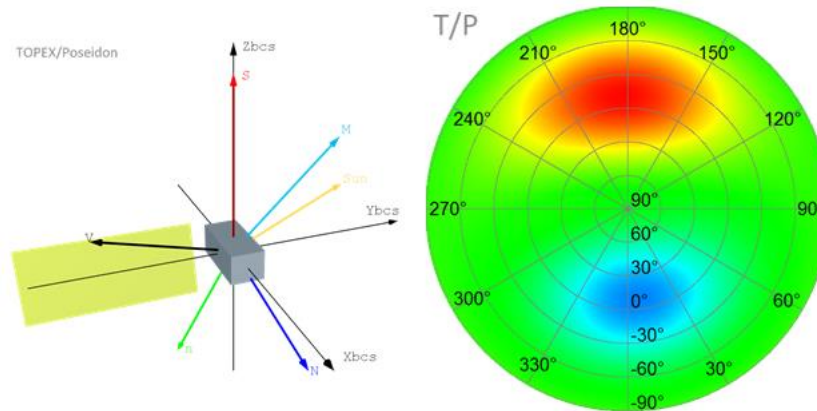
The object characterisation work in RP3 is focused on the dynamics observation, analysis and modelling of the candidates for the SERC laser manoeuvre. The characterisation process is based on the satellite brightness measurements and allows for the determination of the standard magnitude of an object as well as the attitude parameters. The analysis of the observed spin dynamics makes it possible to characterise the interaction between the satellite and the environment. The developed force and torque simulation methods include:

¹ <http://www.industrialsciences.com.au/>, accessed 30-Aug-18.

² <http://www.eos-aus.com/sites/default/files/Space%20Update%201%20August%202018.pdf>, accessed 30-Aug-18.

- space environment models (gravity and magnetic fields of the Earth, solar radiation flux);
- satellite body macromodels (size, center-of-mass, moments of inertia, optical properties);
- satellite attitude models (inertial orientation, spin rate).

An example is provided in Fig. 2 for TOPEX/Poseidon.



- **Fig. 2. Left: TOPEX/Poseidon: satellite body and force vectors. Right: body surface response to the incoming photon flux indicates a larger area where the positive torque can be generated: red) spin-up, blue) de-spin.**

A light curve detector has been developed that will support the space object characterisation and the laser force manoeuvre detection. The unit is designed as a plug-and-play device and measures the intensity of the collected photon flux at the sampling rate of up to 100 kHz. The sunlight reflected from the satellite towards the ground telescope is focused on the photomultiplier module (PMT) Hamamatsu H11901-20 which has a high sensitivity over the entire visible spectrum. The PMT output signal is sampled by the real time processor (PRU) of the Beaglebone PC board and stored in output files. The high rate detector is installed on the A2 telescope (Mount Stromlo) and is currently being tested with various satellites and space debris objects. The high sampling rate allows for the accurate measurement of the very short specular reflections of sunlight from the surface elements of the satellites. The new, fast detectors allow for the development of the high-definition photometry methods that produce satellite reflectivity profiles by correlating high rate brightness observations with the surface reflection point given by the object attitude model. Fig. 3 presents TOPEX/Poseidon reflectivity map measured during a single pass by Graz photon counting system. The intensity of reflection depends on the orientation of the phase vector in the satellite body coordinate system. The high-resolution reflectivity maps will be used to characterise satellites and space debris objects. Details can be found in the paper by Kucharski in this conference.

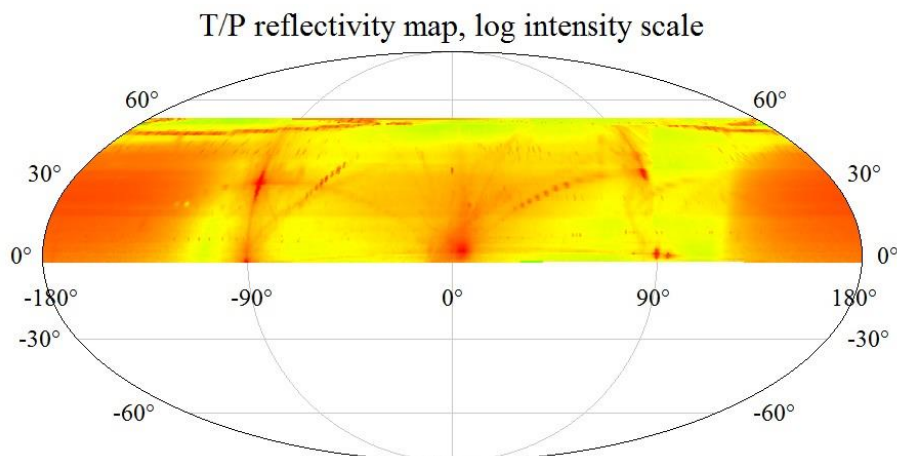


Fig. 3. Reflectivity map of TOPEX/Poseidon measured by Graz photon counting system on July 10, 2015.

A new camera has been deployed to be tested on the A2 telescope for high rate object characterisations in LEO using full frames. An Andor Zyla 5.5 Front Illuminated sCMOS³ camera has just been mounted to the first Nasmyth port, opposite the 100 kHz photo detector on port 2 described above. The Zyla camera is capable of 100 full frames per second and will be used for characterising LEO objects for the manoeuvre campaign.

Objects are also characterised in terms of their physical size/mass attributes. The Ballistic Coefficient Estimation Method [4] is used to estimate the ballistic coefficient of objects in LEO. The method has also been extended to higher altitudes where drag is no longer the dominant non-Gravitational perturbation [5]. These values are used as a priori estimates of the physical characteristics of the objects in the ephemeris generation. During the orbit update step, the ballistic and radiation coefficients are fitted and updated and stored in the database.

6. ORBIT DETERMINATION

Once there is sufficient tracking data on an object an orbit determination is triggered automatically to update the state vector and covariance. A Batch Least Squares method is employed and each object that has sufficient observations is updated. Details of the integrator and the force models employed is shown in Tab. 2.

Tab. 2. Orbit determination settings

Software Language	C++
Integrator	11 th order Störmer-Cowell predictor-corrector
Step size	30 seconds
Forces	Earth Gravity (70 × 70 EGM 96) Earth Tides Lunisolar & planetary gravity General relativity Drag (NRLMSIS-00) Solar radiation pressure Earth radiation pressure Thrust (RTN system)
Satellite body	Spherical/aspherical

Once the orbit determination process has been run, the result is tagged with four possible outcomes:

1. Success – The automated processing is happy with it;
2. Awaiting approval – The automated processing has concerns about some fields, but they might just be absorbing error from other parameters;
3. Quarantine – for manual assessment;
4. Not converged;

The orbit determination process outputs a human readable file with all of the things that were not within bounds for automatic success so a human has an easily read and understood file to make a decision for themselves as to the success of the orbit determination. The automation is undergoing continual improvements but orbital elements have been successfully maintained in all orbital regimes and these have been used to cue the tracking sensors, and in the post-processing and track correlations. These methods benefit greatly from the improved orbital elements and covariance information. The TLE-based methods are less reliable due to their relative inaccuracy.

6.1 Fitting Orbital Manoeuvres

One of the issues that was affecting the orbit determination success was satellites that perform orbital manoeuvres. During the automation active manoeuvring objects were constantly due to tracks being marked as uncorrelated. Improvements are being integrated into the track correlation procedure to identify and correlate tracks for objects undergoing manoeuvres. Manoeuvre detection and resolving is required for objects where the manoeuvre information is not available. SERC is working closely with Optus Satellite Systems and manoeuvre information was provided for their fleet. The orbit determination code was enhanced to fit thrust accelerations and is working well. It can handle small thrust manoeuvres as well as large impulse burns. The thrust accelerations are modelled and fitted

³ <https://andor.oxinst.com/products/scmos-camera-series/zyla-5-5-scmos>, accessed 27-Aug-18.

in the radial, tangential and normal coordinate system. The generic structure that has been used means the method is also applicable to resolving laser-induced manoeuvres.

In the example below, no a priori information was passed to the orbit determination process except for the manoeuvre start and end times. Fig. 4 shows an example of the residuals resulting from fitting 40 days of Optus radio frequency range data, fused with passive optical data from the B3 and B4 sensors. The Optus tracking sensors are located in Sydney and Perth in Australia. These residuals are $n\sigma$ plotted versus time so they can be displayed on the same plot. The σ values for the orbit determination fit for the passive optical data was ~ 0.25 - 0.35 arcsec in the azimuth and elevation for the B3 and B4 systems and ~ 1.4 m for the Sydney and Perth RF sensors.

Now that we have achieved fitting through manoeuvres, the next step is to detect the manoeuvre events and automate this in the orbit determination process. Methods for manoeuvre detection and resolving are in development and will be implemented once proven.

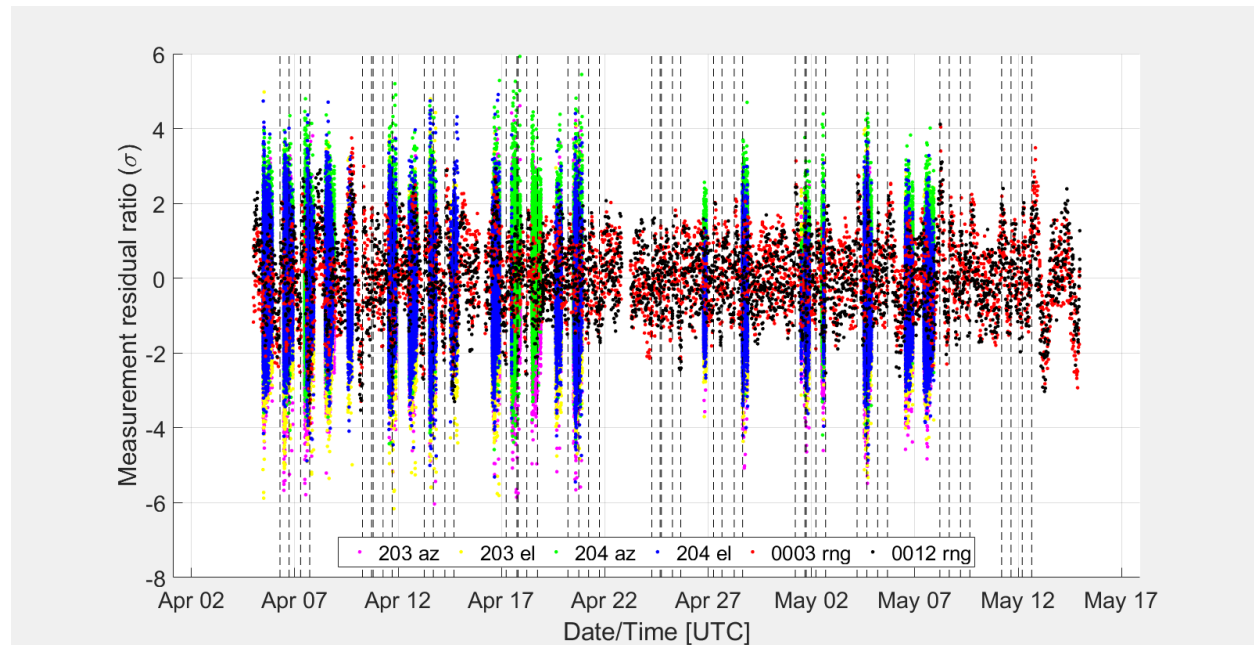


Fig. 4. $n\sigma$ residual plot of a 40 day orbit determination fitting 5 E-W manoeuvres and 49 N-S manoeuvres. Site 203 is B3, 204 is B4 and 0003 and 0012 are the Optus tracking stations located in Sydney and Perth, respectively.

7. CONJUNCTION ASSESSMENTS

The protocols and procedures for sensor tasking after a conjunction assessment have been automated and trials were performed on EOS tracking sensors. This enables rapid response tasking for predicted conjunction events.

The conjunction assessment benefits greatly from the GPU implementation of SGP4. The speedup that has been achieved is shown in Fig. 5. Every night, SERC runs a weekly forecast of close approaches between all objects in the latest public TLE catalogue. All objects are propagated forward for a week with time steps between 60 and 200 seconds. All objects are paired up and run through a chain of pre-filters to determine whether a conjunction is possible. Positive matches are propagated again using smaller time steps to determine the exact time and distance of the closest approach. At a catalogue size of currently approximately 17,000 objects, this results in tens of millions of propagation operations performed as well as hundreds of millions of object pairs checked. Thanks to SGP4 running on the GPU in parallel, propagation of the entire TLE catalogue can now be performed within a few seconds instead of several minutes. The pre-filter chain has been ported to OpenCL as well which contributes to the increased overall performance. Pre-filters currently in use are an apogee/perigee overlap test as described by Hoots et al. [6] as well as a simple Euclidean distance test which, by using the GPU's hardware-intrinsic functions, comes at virtually

no additional computational cost and is able to lower the pass rate from around 36 per cent to under one per cent, resulting in fewer object pairs being selected for additional propagation steps.

A high-accuracy numerical propagator is being optimised for use in extremely accurate conjunction assessments and is currently being parallelised. It has been outfitted with a modern interface and software architecture to facilitate optimisation for parallel computing. Early performance tests indicate that the run time speedup for the numerical propagation will scale (almost perfectly) linearly with the number of objects suggesting it will scale well on GPUs with thousands of cores.

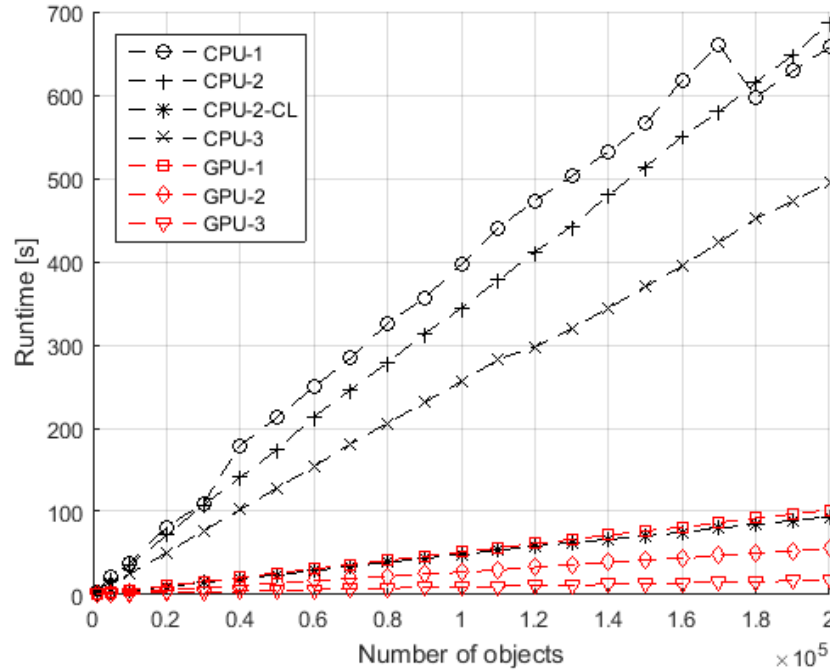


Fig. 5. The total runtime for a 7 day propagation versus the number of objects in the catalogue comparing several CPUs and GPUs. The equipment key is as follows: CPU-1 = Intel i7-4710HQ 3.5GHz (one core); CPU-2 = Intel Xeon E5-1620 3.6GHz (one core); CPU-2-CL = Intel Xeon E5-1620 3.6GHz (OpenCL, 8 cores); CPU-3 = Intel i7-7700 3.6GHz (one core); GPU-1 = Nvidia GeForce 860m (OpenCL); GPU-2 = Nvidia GeForce GTX960 (OpenCL); GPU-3 = Nvidia GeForce GTX1070 (OpenCL)

8. STATE UNCERTAINTY PREDICTION⁴

The focus of past research has been to establish rigorous methods for state uncertainty prediction and collision likelihood estimation. Using the particle method approach in combination with two-body motion, fundamental relations between initial states, covariances and the uncertainty volume evolution have been studied. An emphasis has been put on rigorous assessment of the breakdown of normality of the state uncertainty in position as well as position + velocity via the Henze-Zirkler (HZ) test for multivariate normality (MVN) [7]. The HZ test metric falls into the category of “consistent approaches” [8]. The test was chosen due to its relatively low Type I error rate of about 5% as well as its robustness. Using this approach a common structure has been found to underlie the time evolution of this metric from Gaussian to non-Gaussian uncertainty distributions. Fig. 6 shows an example evolution of the metric for the position uncertainty for three different initial random samples. The evolution can be split roughly into three stages: i) Fully Gaussian; ii) Partially Gaussian; iii) Fully Non-Gaussian. During the initial phase following the state epoch, the uncertainty remains Gaussian throughout the entire orbit. During this stage, type I error causes some samples to still flag non-Gaussianity. The uncertainty volume then becomes non-Gaussian during parts of the orbit. During this phase, a common structure materialises between the time-evolution of all initial samples until, in the final phase, all samples exhibit the same time evolution and the uncertainty volume is non-

⁴ Some of the detail in the section is given in the companion-paper by Sven Flegel “Normality in State Uncertainties from Orbit Determination Results fitting Optical Measurements”

Gaussian throughout the entire orbit. Generally, the six dimensional position + velocity uncertainty space has been found to be better behaved than the three dimensional position-only uncertainty. Furthermore, the position uncertainty has a strong half-orbit periodicity while the position + velocity uncertainty exhibits a full orbit periodicity. Finally it is observed that the position + velocity uncertainty remains Gaussian for a much shorter time than the position uncertainty.

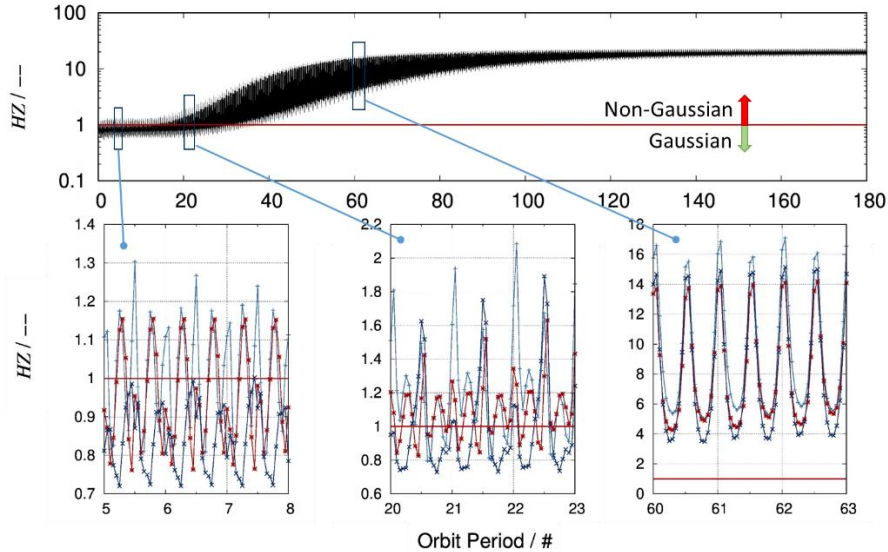


Fig. 6. Time evolution of the normalised Henze-Zirkler (HZ) test statistic for Multivariate Normality. MVN Breakdown occurs in three stages: i) Fully Gaussian, ii) Partially Gaussian, iii) Fully Non-Gaussian.

8.1 Conjunction Probability Assessment

Using the established particle approach, different close encounter geometries in GEO as well as relation between hard-body radius, uncertainty size and miss distance have been studied. An assessment using the European Space Agency's MASTER-2009 model has shown about 60 % of close encounters in GEO may be expected to involve objects on libration orbits with encounter velocities up to ~800 m/s. The majority of the remaining encounters involve objects on GEO drift orbits where encounter velocities up to 3 km/s have been estimated, but the average value is below 1 km/s. The remaining 3 % of encounters involve objects with encounter velocities above 1 km/s. Fig. 7 shows the evolution of the probability of collision as well as heat-maps of the time-of-closest-approach (TCA) of pairs of particles generated from the state uncertainties. The case numbers refer to those published in [9]. It can be seen that the miss-distance distribution is highly non-Gaussian and depends greatly on the uncertainty size as well as the relative motion.

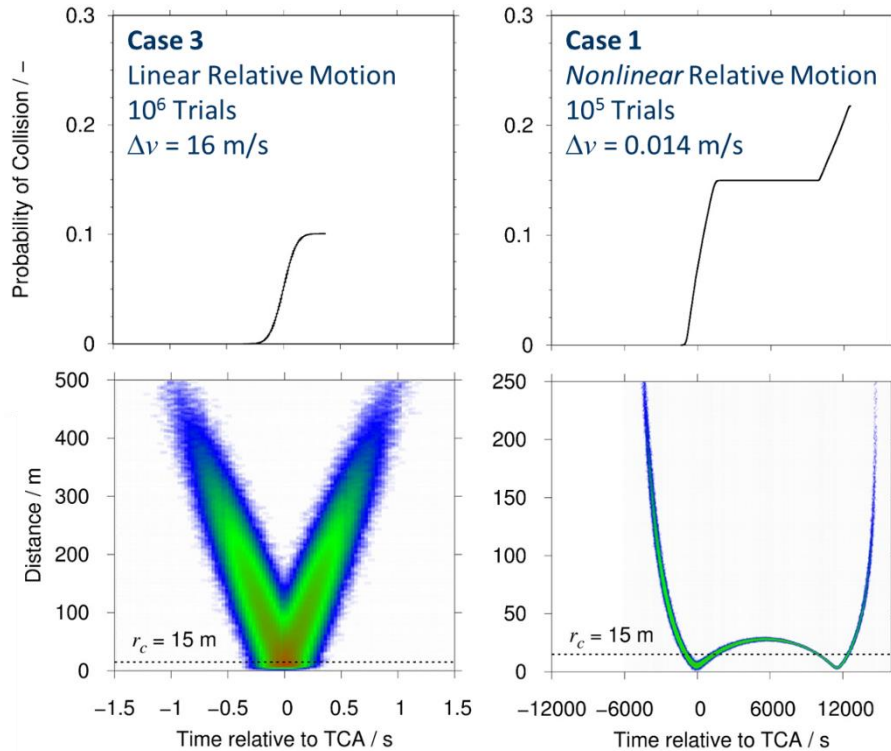


Fig. 7. Top: Time evolution of probability of collision for combined hard-body radius of $r_c = 15$ m. Bottom: Heat maps of distance of each trial at its respective time of closest approach (TCA). The dashed lines indicate the hardbody radius. Figures taken from⁵.

Work is currently underway to use the knowledge gained from the MVN Breakdown analyses to incorporate this information into SERC's object catalogue. This information would then be used to inform other methods employing predictions of the state uncertainty including assessments of the conjunction probability. It is planned to test first operational methods for conjunction probability assessment later this year.

In the following Section, detail on other research being performed in RP3 that is currently not being integrated into the CATW service. This research forms the educational component of RP3 and SERC is supporting PhD research throughout all of their research programs.

9. OTHER RESEARCH

Joseph O'Leary is a final year PhD student at the University of South Australia. His primary research focus is the inclusion of general relativity within the space sciences. For the study of near-Earth objects, such as navigation or geodetic satellites; the inclusion of general relativity is achieved using the first post-Newtonian approximation. With the increasing technological advances and higher demand for accuracy in orbit determination software, Joseph researches potential improvements to the IERS-recommended post-Newtonian equations of motion. Further, Joseph is concerned with the overall dynamics of objects within the post-Newtonian regime. To date, we have derived a new energy integral associated with near-Earth objects [10]. The Jacobi-like integral has the potential to be used in components of geodesy such as improved gravity field determination. Further, Joseph has derived a new post-Newtonian satellite orbit equation which more accurately resembles general relativistic orbits [11]. The final stages of Joseph's PhD research will be developing new post-Newtonian planetary/satellite perturbation equations consistent with his new results.

Hansani Thanippuli Kankanamalage is studying the mathematical modelling of collision probabilities for LEO short-term encounters. These encounters can occur in any orbit but often take place in the LEO environment due to

⁵ Flegel S., Towards state uncertainty accuracy requirements for actionable GEO collision risk assessments

high relative velocities. A standard approach for modelling short-encounter probabilities is based on a three-dimensional Gaussian probability density for the position uncertainty of two objects. With the assumption of rectilinear and constant relative velocity for the two space objects at the time of closest approach, the three dimensional problem can be reduced to the integration of a two dimensional Gaussian probability density of the combined error ellipsoid over the hard-body circle. However, to account for data that contains outliers another distribution with heavier or thicker tails is required. Also it has been shown that the position uncertainty of a space object at the epoch is reasonably Gaussian but becomes non-Gaussian as neglecting nonlinearities in the covariance prorogation [12]. We model the position uncertainty of two objects using a three dimensional Generalized Gaussian Distribution (GGD) with the probability density given below:

$$f_{\mathbf{x}}(\mathbf{x}|\boldsymbol{\mu}, \boldsymbol{\Sigma}, \beta) = \frac{3}{\pi\Gamma\left(1 + \frac{3}{2\beta}\right) 2^{1+\frac{3}{2\beta}}} |\boldsymbol{\Sigma}|^{-\frac{1}{2}} \exp\left\{\frac{-[(\mathbf{x} - \boldsymbol{\mu})^T \boldsymbol{\Sigma}^{-1}(\mathbf{x} - \boldsymbol{\mu})]^\beta}{2}\right\}.$$

The three dimensional GGD allows for extreme values to be included in the modelling as distributions with shape parameter $\beta \leq 0.5$ have heavy tails. Therefore, it can be used rigorously when outliers (or less accurate sources of information) are present in the data and may provide accurate results efficiently during initial stages of the breakdown of Gaussianity. The GDD allows for modelling the error distribution using the L_1 -norm distribution [13], and the Huber distribution – which is a mixture model method using L_1 -norm and L_2 -norm [14]. Setting $\beta = 0.5$ and $\beta = 1$ results in the L_1 -norm and L_2 -norm distributions, respectively. Also it explains Gaussian family of distributions when $\beta = 1$ and the set of possible symmetric distributions for position uncertainty for $\beta \in (0, \infty)$ [15].

Richard Samuel is developing methods and evaluation strategies for forming a multivariate optimisation problem to synthesise drag and solar radiation pressure characteristics for selected objects, using accepted geophysical and atmospheric density models. This has the possibility of also revealing their time-varying nature, as well as identifying non-natural forces if they are apparent. As opposed to methods that fuse direct observables in the characterization process, numerical synthesis methods will be used to explore candidate objects and trajectories. Historical known conjunction events will be used to test the method, employing a forensic analysis to assess the null hypothesis of a conjunction event, or reject it. This research is relevant to the SERC in its effort of refining the characteristics of space objects for enhanced orbital conjunction assessments.

10. TIMELINE FOR FULL OPERATIONAL CAPABILITY

The process of bringing together wide areas of research into an operational CATW system is time consuming. Given the importance of its function in supporting the laser manoeuvre campaign and satellite operator conjunction warnings, accurate and actionable knowledge must be produced. This is a strong focus of the implementation of the system.

The timeline for initial operational capability is November 2018 where Conjunction Data Messages will be produced and sent to Optus for comparison with JSpOC predictions. Full operational capability will follow soon after in early 2019 to be ready for SERC's laser manoeuvre campaign.

11. ACKNOWLEDGEMENTS

The authors would like to acknowledge the support of the Cooperative Research Centre for Space Environment Management (SERC Limited) through the Australian Government's Cooperative Research Centre Programme. The authors would also like to thank Optus' staff for their support in the conjunction and threat warning service development and the orbital dynamics of thrust manoeuvres. Also thank you to Dr Steve Gehly for his work on the information gain based scheduler at SERC.

REFERENCES

1. Yue, G., et al., *High average power diode pumped solid state laser*. Laser Physics Letters, 2017. **14**(3): p. 035803.
2. Gehly, S. and J. Bennett, *Incorporating Target Priorities in the Sensor Tasking Reward Function*, in *Advanced Maui Optical and Space Surveillance Technologies Conference*. 2015: Maui, Hawaii.

3. Gehly, S. and J. Bennett, *Distributed Fusion Sensor Networks for Space Situational Awareness*, in *68th International Astronautical Congress*. 2017: Adelaide, Australia.
4. Sang, J., J.C. Bennett, and C.H. Smith, *Estimation of ballistic coefficients of low altitude debris objects from historical two line elements*. *Adv. Space Res.*, 2013. **52**(1): p. 117-124.
5. Bennett, J.C., et al., *Orbital element generation for an optical and laser tracking object catalogue*, in *Advanced Maui Optical and Space Surveillance Technologies Conference*. 2015: Maui, Hawaii.
6. Hoots, F.R., L.L. Crawford, and R.L. Roehrich, *An analytic method to determine future close approaches between satellites*. *Celestial Mechanics*, 1984. **33**(2): p. 143-158.
7. Henze, N. and B. Zirkler, *A class of invariant consistent tests for multivariate normality*. *Communications in Statistics - Theory and Methods*, 1990. **19**(10): p. 3595-3617.
8. Mecklin, C.J. and D.J. Mundfrom, *A Monte Carlo comparison of the Type I and Type II error rates of tests of multivariate normality*. *Journal of Statistical Computation and Simulation*, 2005. **75**(2): p. 93-107.
9. Alfano, S., *Satellite conjunction Monte Carlo analysis*. *Advances in the Astronautical Sciences*, AAS09-233, 2009. **134: 2007-2024**.
10. O'Leary, J., J.M. Hill, and J.C. Bennett, *On the energy integral for first post-Newtonian approximation*. *Celestial Mechanics and Dynamical Astronomy*, 2018. **130**(7): p. 44.
11. O'Leary, J. and J.M. Hill, *Post-Newtonian satellite orbits: submitted for publication*. *Astrophysics and Space Sciences*, 2018.
12. Alfriend, K.T. and I. Park, *When does the uncertainty become non-Gaussian*, in *Advanced Maui Optical and Space Surveillance Technologies Conference*. 2016: Maui, Hawaii.
13. Gehly, S., J. Bennett, and M. Afful, *Lp-Norm Batch Estimation As Applied To Orbit Determination*, in *AIAA/AAS Astrodynamics Specialist Conference*. 2016, American Institute of Aeronautics and Astronautics.
14. Gehly, S., et al., *Minimum L1 norm orbit determination using a sequential processing algorithm*, in *Advances in the Astronautical Sciences*. 2012. p. 1457-1473.
15. Gómez, E., M.A. Gomez-Viilegas, and J.M. Marín, *A multivariate generalization of the power exponential family of distributions*. *Communications in Statistics - Theory and Methods*, 1998. **27**(3): p. 589-600.